Periodica Polytechnica
Civil Engineering

61(3), pp. 483–490, 2017
https://doi.org/10.3311/PPci.8717

Evaluation of the Warping Model for Analysis of Polystyrene Concrete Slabs with Profiled Steel Sheeting

Volodymyr Cherednikov[1], Olena Voskobiinyk[2], Oleksandra Cherednikova[2*]

RESEARCH ARTICLE

Received 24 October 2015; Revised 05 January 2016; Accepted 15 March 2016

Abstract

In this article the possibility of applying the warping model offered by V. G. Piskunov, A. V. Goryk and V. N. Cherednikov for analyzing polystyrene concrete slabs with profiled steel sheeting is considered. The adequacy of the offered model was verified by comparing the experimental and calculated deflections of the slab. Test specimens of polystyrene concrete slabs with profiled steel sheeting (PCSPSS) were made for experimental studies and then mechanical properties of the slab components – the polystyrene concrete and the profiled steel sheeting – were determined. Then the behaviour of slabs under a load was studied. The calculation of the warping model of PCSPSS was done at the same time. The obtained results have proved the possibility of applying of the offered warping model for analysis of PCSPSS. It is proposed to use the considered model for further study of the stress-strained state of inhomogeneous slabs.

Keywords

Polystyrene concrete slabs, profiled steel sheeting, warping model, transverse shear, inhomogeneous cross-section, flat cross-section hypothesis

[1] Chief Designer Department
DB Aerocopter Ltd
52, Zinkivska St.
Poltava, Ukraine
[2] Architecture and Urban Construction Department,
Poltava National Technical Yuri Kondratyuk University,
24, Pershotravnevyi avenue
Poltava, Ukraine
* Corresponding author e-mail: polvl@yandex.ua

1 Introduction

Composite structures based on light concretes with profiled steel sheeting have been widely applied recently, especially in construction. Most often, these structures are used as lapping in construction of new low-rise buildings as well as in reconstruction of the existing buildings. The use of the light concretes with profiled steel sheeting ensures several advantages, such as the possibility of slab production directly on a building site, structure lightweight and its sufficient strength. However, one of the main problems which limits the application of concrete structures with profiled sheeting is the absence of a sufficiently reliable method for its analysis.

The accounting for a combined action of sheeting and concrete, as well as the determination of the moment of their separation and the coming loss of load-carrying capability of the slab are the most difficult and interesting tasks here. Since separation of the profiled sheeting from the concrete occurs due to transverse stresses at the boundary of contacting materials, determination of the transverse stresses is the main task of such a method. Herewith, shear deformations should be taken into account as they cause cross-section warping. One of the models which combines all those features is a model developed by V. G. Piskunov and co-authors. Accounting for inhomogeneous structure of the cross-section is a distinctive feature of this model. Existing models [1–10] are used for analyzing layered beams and slabs with a simple cross-sectional shape without inclusions, so the considered model enables us to take into account any inhomogeneous structure of cross-section. However, this model has not yet been applied for analyzing reinforced concrete structures.

To assess the applicability of checking and verify the model, offered by V. G. Piskunov and co-authors in [11–13] for studying steel reinforced concrete structures, it is necessary to carry out an analysis of a real structure, and to compare the obtained results with the experimental data. To do so, a polystyrene concrete slab with profiled steel sheeting (PCSPSS) for which experimental results were known has been taken as the object of research.

2 Determination of mechanical properties of the profiled steel sheeting and the polystyrene concrete

The mechanical properties of the profiled steel sheeting were determined by testing of three strip specimens (Fig. 1 and Fig. 2). The test specimens were cut from the web of the profiled steel sheeting. The specimen dimensions are shown below:

b_o = 20 mm – specimen width;
l_o = 60 mm − initial length;
l = 100 mm − working length;
h_1 = 50 mm – grip length;
$L = l + 2h_1$ =200 mm – specimen full length.

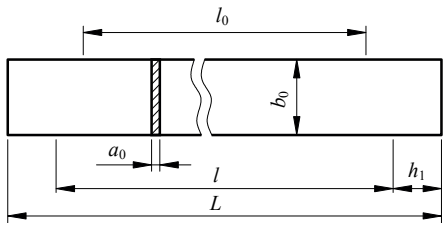

Fig. 1 Strip specimen dimensions

Fig. 2 Steel strip testing

The mechanical properties of the profiled steel sheeting are given in Table 1.

Table 1 The mechanical properties of steel of the profiled sheeting

The modulus of elasticity (MPa)	The yield strength (MPa)	The ultimate strength (MPa)
2.1×10^5	332	355

The mechanical properties of the polystyrene concrete were determined by testing of the prisms and the cubes. The concrete elasticity modulus was determined by testing of 300 × 100 × 100 mm prismatic specimens (Fig. 3), and the concrete strength was determined by testing of 100 × 100 × 100 mm cubic specimens (Fig. 4). The polystyrene concrete consists of:

– portland cement (class 52.5) – 200 kg;
– polystyrene (diameter 4–6 mm) – 1.05 m^3;
– liquid air entraining admixture – 1.0 kg;
– water – 100 l.

The concrete specimens were visually inspected for defects. The maximum testing force is assumed to be a failure load.

Fig. 3 The prismatic concrete specimens

Fig. 4 The strength test of the polystyrene concrete cubs

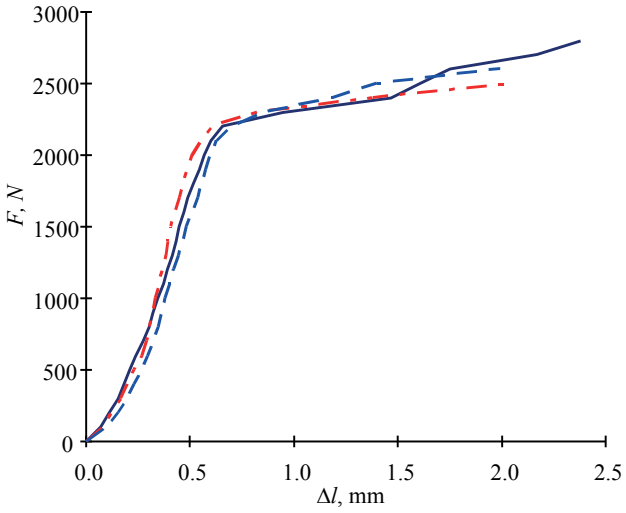

Fig. 5 The deformation curves of the prismatic specimens

The deformation curves of three prismatic specimens are shown in Fig. 5. According to these diagrams, the maximum load for determination of the concrete modulus of elasticity shall not exceed 2000 N.

The cubic specimens in the polystyrene concrete strength test and its failure are shown in Fig. 4. The test results for the cylindrical and cubic specimens are given in Table 2.

Table 2 The mechanical properties of the polystyrene concrete

Density (kg/m^3)	The modulus of elasticity (MPa)	Bearing capacity (kN)	The ultimate strength (MPa)
335	70	7.3	73

3 Testing of slab in bending

The single-span slabs with span length l = 1.5 m were tested (see Fig. 6). The static load as the metal cylinders was applied to the polystyrene concrete slabs through the wooden plank incrementally. The plank spacing was l/4 (see Fig. 6 and Fig. 7). The load remains unchanged during 5–10 minutes at each step.

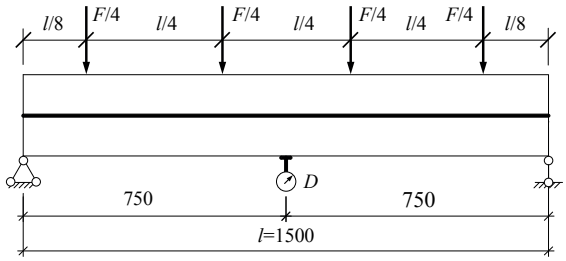

Fig. 6 The gages location scheme: *D* – indicating gage for deflection measurement (deflectometer)

Fig. 7 Test specimen – the polystyrene concrete slab with profiled steel sheeting

The total applied load was equal 12666 N. Herewith the slabs were not adjusted to structural failure. The deflectometer was located at a mid-span. Additionally, the shear deformation between the polystyrene concrete and the profiled steel sheeting was measured in the tests. The gages location scheme is shown in Fig. 6. The testing results are given in Table 3 and Fig. 17.

Table 3 Experimental deflections of the polystyrene concrete slab with profiled steel sheeting

Load step	Load (kN)	Deflection (mm)	Load step	Load (kN)	Deflection (mm)
0	0.000	0.00	7	10.418	4.85
1	1.835	1.03	8	10.866	5.08
2	3.616	1.83	9	10.866	5.27
3	5.419	2.55	10	11.768	5.50
4	7.205	3.32	11	12.666	5.85
5	9.061	4.04	12	12.666	6.00
6	9.965	4.47			

Specific crackle was heard during the eighth load step and the webs of the profiled steel sheeting started delaminating from the concrete. During the 10 and 12 load steps the crackle was increasing, the flanges of the profiled steel sheeting were delaminated from the concrete. After the profiled steel sheeting had been delaminated from the concrete, the combined action of both was not ensured.

4 Classical and non-classical warping models

A slab with an inhomogeneous structure of a cross-section is considered. The design of the slab and the example of the cross-section division into areas are shown in Fig. 8 and Fig. 9. The algorithm of the cross-section preparation for the analysis of the slab was studied in [14].

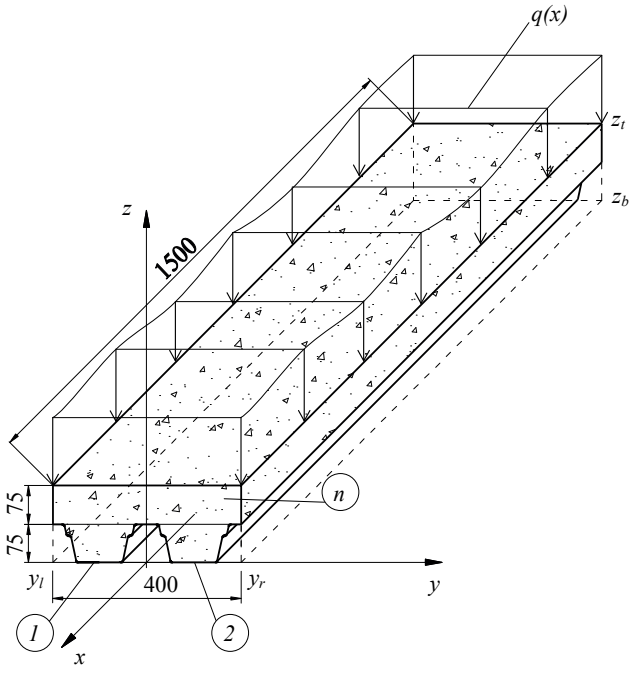

Fig. 8 The design of the polystyrene concrete slab with profiled steel sheeting (dimensions in mm)

Thus, the elastic and the shear modulus were defined as:

$$E(y,z)=\sum_{k=1}^{n}E_k\left\{\theta(y-y_{l_k})-\theta(y-y_{r_k})\right\}\cdot\left\{\theta(z-z_{b_k})-\theta(z-z_{t_k})\right\};$$
$$\frac{1}{G(y,z)}=\sum_{k=1}^{n}\frac{1}{G_k}\left\{\theta(y-y_{l_k})-\theta(y-y_{r_k})\right\}\cdot\left\{\theta(z-z_{b_k})-\theta(z-z_{t_k})\right\}, \quad (1)$$

where Ek, Gk, – the elastic and the shear modulus of the *k*th area;

n – the number of areas;

$\theta(z)$, $\theta(y)$ – generalized Heaviside step function:

$$\theta(y)=\begin{cases}0, y\le 0\\ 1, y>0\end{cases}; \qquad \theta(z)=\begin{cases}0, z\le 0\\ 1, z>0\end{cases}; \quad (2)$$

In our case a classical model is the model based on the flat cross-section hypothesis. The classical model quantities were denoted by the index «0», and non-classical warping model quantities – by the index «1».

Therefore, the formulas of the normal stresses and the transverse stresses for the classical model in case of transverse bending were defined as:

$$\sigma_x^{(0)}(x,y,z)=\frac{d^2w(x)}{dx^2}E(y,z)\xi_0(z) \quad (3)$$

$$\tau_{xz}^{(0)}(x,z)=\frac{d^3w(x)}{dx^3}f_0(z) \quad (4)$$

where $w(x)$ – deflection function,

$$\xi_0(z)=\frac{B_0(z_t)}{B(z_t)}-\psi_0(z) \quad (5)$$

$$\psi_0(z)=z-z_b \quad (6)$$

$$B(z)=\int_{z_b}^{z}\int_{y_l}^{y_r}E(y,z)dydz \quad (7)$$

$$B_0(z)=\int_{z_b}^{z}\int_{y_l}^{y_r}E(y,z)\psi_0 dydz \quad (8)$$

$$f_0(z)=\frac{1}{b(z)}\left(B_0(z)-\frac{B_0(z_t)}{B(z_t)}B(z)\right) \quad (9)$$

where b(z) – width of the cross-section at the ordinate *z*.

The construction of the non-classical warping model assumes the existence of the self-balanced stress state, in which the transverse stresses were defined as:

$$\tau_{xz}=\frac{d\chi}{dx}f_0(z) \quad (10)$$

Where the shear function $\chi(x)$ was introduced in irreversible conformity:

$$\frac{d^3w(x)}{dx^3}\Rightarrow\frac{d\chi(x)}{dx} \quad (11)$$

Then, the normal and the transverse stresses of the warping model were equal, respectively:

$$\sigma_x^{(1)}(x,y,z)=E(y,z)\left(\frac{d^2w(x)}{dx^2}\xi_0(z)-\frac{d^2\chi(x)}{dx^2}\xi_1(z)\right) \quad (12)$$

$$\tau_{xz}^{(1)}(x,y,z)=\frac{d^3w(x)}{dx^3}f_0(z)-\frac{d^3\chi(x)}{dx^3}f_1(z) \quad (13)$$

where

$$\xi_1(z)=\frac{B_1(z_t)}{B(z_t)}-\psi_1(z) \quad (14)$$

$$\psi_1(z)=\frac{1}{b(z)}\int_{z_b}^{z}\int_{y_l}^{y_r}\frac{f_0(z)}{G(y,z)}dydz \quad (15)$$

$$B_1(z)=\int_{z_b}^{z}\int_{y_l}^{y_r}E(y,z)\psi_1(z)dydz \quad (16)$$

$$f_1(z)=\frac{1}{b(z)}\left(B_1(z)-\frac{B_1(z_t)}{B(z_t)}B(z)\right) \quad (17)$$

Expanded formulas for the functions $\Psi_1(z)$ and $B_1(z)$ were given in [14].

The deflection function $w(x)$ and the shear function $\chi(x)$ were determinated from the next system of equation taking into account the boundary condition [14]:

$$\begin{cases}D_{00}\dfrac{d^4w(x)}{dx^4}+D_{01}\dfrac{d^4\chi(x)}{dx^4}=q(x)\\ D_{10}\dfrac{d^4w(x)}{dx^4}+D_{11}\dfrac{d^4\chi(x)}{dx^4}-D_{10}\dfrac{d^2\chi(x)}{dx^2}=0\end{cases} \quad (18)$$

where D_{00}, D_{01}, D_{10}, D_{11}, the cross-section stiffness constants.

A solution of the system (18) was given in [12] and [13].

The cross-section stiffness constants are determined for both a classical model and a warping model. They were given by:

$$D_{00}=\frac{B_0^2(z_t)}{B(z_t)}-D_{00}^* \quad (19)$$

$$D_{01}=\frac{B_0(z_t)B_1(z_t)}{B(z_t)}-D_{01}^* \;;\; D_{01}=D_{10} \quad (20)$$

$$D_{11}=\frac{B_1^2(z_t)}{B(z_t)}-D_{11}^* \quad (21)$$

where

$$D_{00}^*=\int_{y_l}^{y_r}\int_{z_b}^{z_t}E(y,z)\psi_0^2(z)dzdy \quad (22)$$

$$D_{01}^{*} = \int_{y_l}^{y_r}\int_{z_b}^{z_t} E(y,z)\psi_0(z)\psi_1(z)dydz \tag{23}$$

$$D_{11}^{*} = \int_{y_l}^{y_r}\int_{z_b}^{z_t} E(y,z)\psi_1^2(z)dydz \tag{24}$$

In this case the cross-section was divided onto 14 areas (Fig. 9). The material of the profiled steel sheeting (areas 1, 2, 3, 5, 6, 8, 9, 11, 13) was galvanized steel with the elastic modulus $E = 2.1 \times 10^{11}$ Pa and the shear modulus $G = 0.8 \times 10^{11}$ Pa. The material of areas 4, 7, 10, 12, 14 was polystyrene concrete with the elastic modulus $E = 70 \times 10^{6}$ Pa and the shear modulus $G = 31.8 \times 10^{6}$ Pa. The slab was simply supported. The loading was uniformly distributed over the top surface of the slab and its magnitude was equal to 8444 N/m.

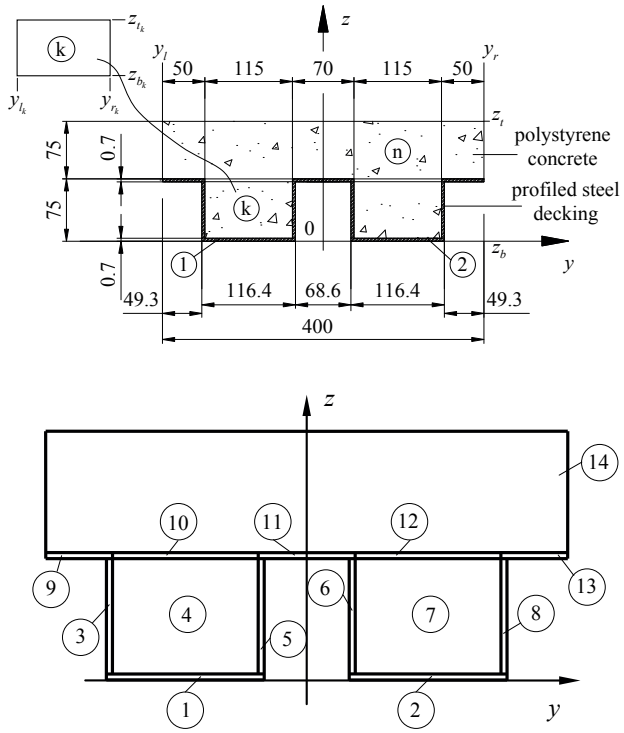

Fig. 9 An approximated cross-section of the slab and its division into areas (dimensions in mm)

As a result, the next values were obtained for the approximated cross-section (see Fig. 9):

$$D_{00} = 1.5304 \cdot 10^{5}\ \text{N}\times\text{m2},$$

$$D_{01} = 3.8684 \cdot 10^{4}\ \text{N}\times\text{m}^4,$$

$$D_{11} = 1.0022 \cdot 10^{4}\ \text{N}\times\text{m}^6.$$

5 Results and discussion

After determination of the cross-section stiffness constants, the slab stresses and displacements were analyzed. A slab deflection according to a flat cross-section hypothesis and the warping model are shown in Fig. 10. The maximum deflections were equal 3.7 and 6.6 mm, respectively. It is clear that warping influences the slab deformed state and increases the deflection by a factor of 6.6 / 3.7 = 1.78 .

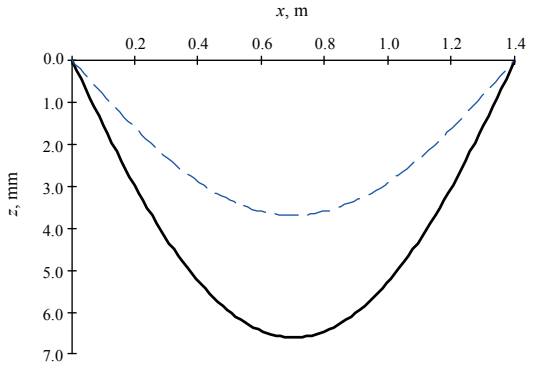

Fig. 10 Comparison of the deflections predicted by the model based on the flat cross-section hypothesis (dashed line) and the warping model (full line)

The effect of warping on the stress state of polystyrene concrete and profiled steel sheeting is shown in Fig. 11 – Fig. 13. A common feature in changing of the stress state is that a redistribution of the normal and transverse stresses is caused by a transverse shear. The stresses in a metal are decreased insignificantly but in a concrete they increased significantly larger. Distribution of the normal stresses over the entire length of the slab is shown in Fig. 11 and Fig. 12.

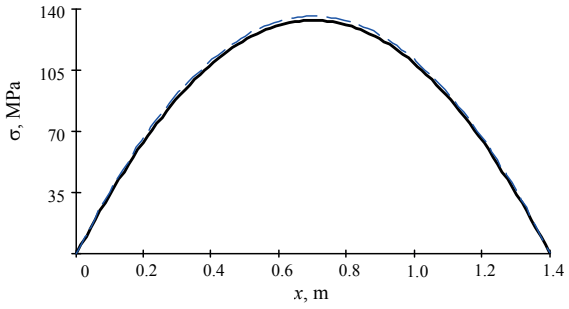

Fig. 11 Trough-length distribution of normal stresses for the bottom point of the cross-section in profiled steel sheeting

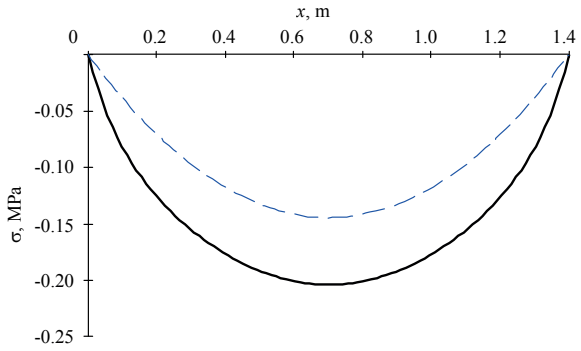

Fig. 12 Through-length distribution of normal stresses for the top point of cross-section in polystyrene concrete

The distribution of the normal stresses at the leftmost edge is illustrated in Fig. 13a (y = -0.2 m). The stress discontinuity refers to the profiled steel sheeting, where the stresses reach 143 MPa. The through-thickness distribution of the normal stresses in polystyrene concrete is shown in Fig. 13b in the expanded scale.

The normal stresses of the cross-sections at y = -0,1507 m and y = -0,1 m, respectively, are illustrated in Fig. 13c and Fig. 13d. Fig. 13c also indicates the position of the neutral line, where normal stresses move from the tensile to the compression zone. The stresses discontinuity at z = 0,075 m (Fig. 13d) refers to the upper surface of the profiled steel sheeting. This discontinuity is predicted by the non-classical model only. There is no such discontinuity in analyses based on a flat cross-section hypothesis (dashed line).

The shear warping has a negligible effect on stress-state of the profiled steel sheeting; however, it significantly increases the normal stresses in polystyrene concrete – from 0,145 MPa to 0,204 MPa, which is illustrated in Fig. 11 – Fig. 13.

The distribution of maximum transverse stresses over the entire length of the slab is shown in Fig. 14 and Fig. 15.

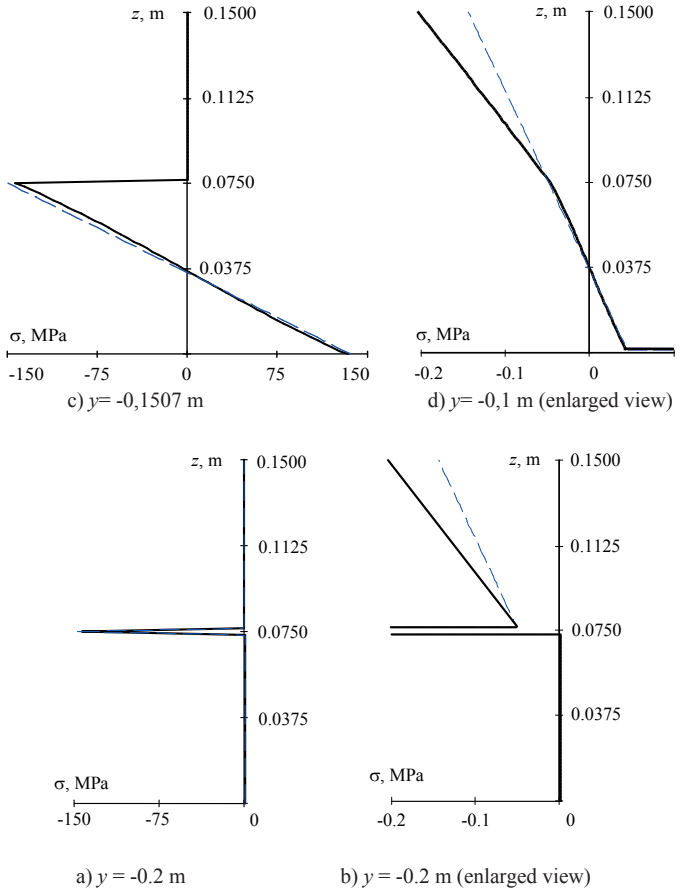

Fig. 13 Through-thickness distribution of the normal stresses in the middle of the slab span

The shear warping has the same effect on the distribution of transverse stresses as it has on the distribution of the normal stresses. As it can be seen in Fig. 14 and Fig. 15, the behaviour of transverse stresses differs from the classical model in the supporting areas. Similar results were obtained by Poonam Kumari, Santosh Kapuria and R.K.N.D. Rajapakse in [15]; Y.–Y. Su, X–L. Gao in [16]; X. Wang, G. Shi in [17] and other authors [18]–[21]. The nature of this phenomenon is explained in Fig. 16. Transverse stresses are decreased at the neutral line ($z \approx 0.0375$ m) and increased on the upper surface of the profiled steel sheeting (z = 0.0750 m). It should also be mentioned that non-classical and classical models produce the same bending moments and shear forces in spite of the differences in stress distribution.

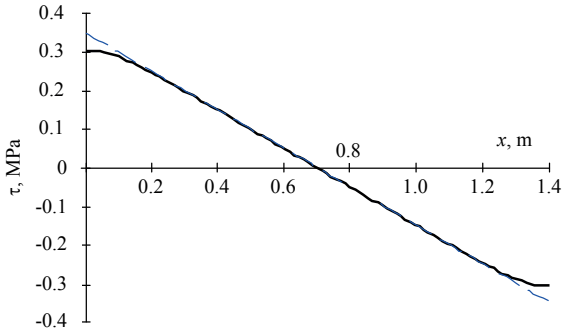

Fig. 14 Trough-length distribution of transverse stresses at z=0.0375 m

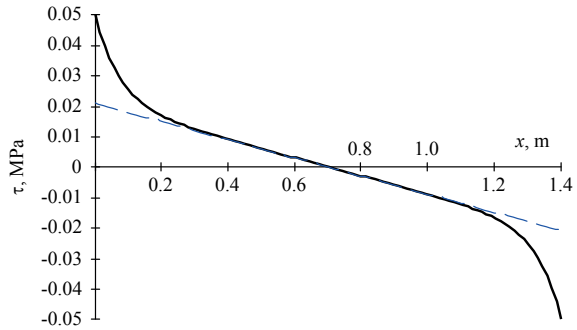

Fig. 15 Trough-length distribution of transverse stresses at z=0.0750 m

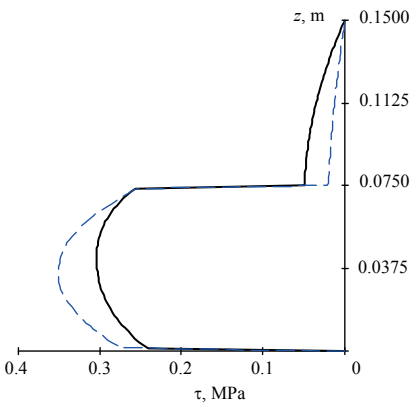

Fig. 16 Trough-thickness distribution of transverse stresses

The shear has more effect on transverse stresses than it has on normal stresses. Transverse stresses are increased more than twice as much in the middle of the thickness.

6 Validation of the proposed model through the experimental test

Comparison of the experimental data and the analysis results shows that the analysis based on a flat cross-section hypothesis gives considerably smaller deflections than experimental deflections (Fig. 17). The deflections predicted by the warping model provide a good approximation with testing results. It is proved that the warping model can be practically applied for analysis of the PCSPSS. The deflections of the PCSPSS are shown in Table 4.

Table 4 Max deflections of the polystyrene concrete slab with profiled steel sheeting

Experimental (mm)	Theoretical (mm)	
	A flat cross-section hypothesis	A warping model
5.8	3.7	6.0

7 Conclusions

The above analysis proves the possibility of applying the warping model for accurate prediction of the monolithic PCSPSS behaviour.

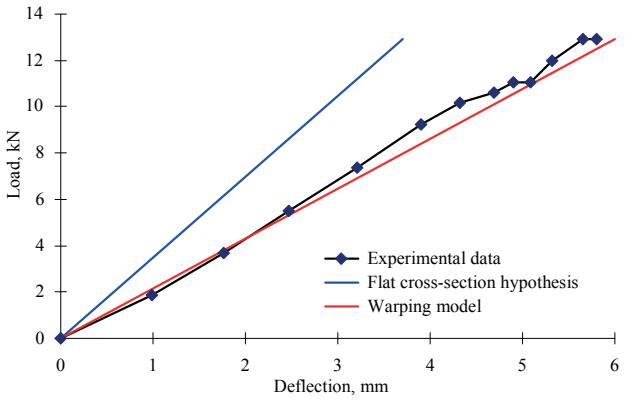

Fig. 17 Comparison of the experimental data and analysis results

The obtained results revealed the new features of the stress-strained state of inhomogeneous slab. These features are caused by the shear deformation and have a significant affect on the strength and deformation of the whole plate.

Acknowledgement

Authors are obliged to the Poltava National Technical Yuri Kondratyuk University for the technical support. Special thanks to Dr. Oleksander Semko for his valuable assistance during the experiments.

References

[1] Timoshenko, S. "*Theory of elasticity*." New York: McGraw-Hill Book Company, Inc., 1934.

[2] Reissner, E. "On transverse bending of plates, including the effect of transverse shear deformation." *International Journal of Solids and Structures*. 11, pp. 569–573. 1975. https://doi.org/10.1016/0020-7683(75)90030-X

[3] Whitney, J., Pagano, N. "Shear deformation in heterogeneous anisotropic plates." *Journal of Applied Mechanics*. 37, pp. 1031–1036. 1970. https://doi.org/10.1115/1.3408654

[4] Reddy, J. "A refined nonlinear theory of plates with transverse shear deformation." *International Journal of Solids and Structures*. 20(9), pp. 881–896. 1983. https://doi.org/10.1016/0020-7683(84)90056-8

[5] Khdeir, A., Reddy, J., Librescu, L. "Analytical solution of a refined shear deformation theory for rectangular composite plates." *International Journal of Solids and Structures*. 23(10), pp. 1447–1463. 1986. https://doi.org/10.1016/0020-7683(87)90009-6

[6] Reddy, J. "*Mechanics of laminated composite plates and shells*." 2nd ed. Boca Raton, Florida, USA, CRC Press LLC, 2004.

[7] Carrera, E. "Developments, ideas and evaluations based upon Reissner's mixed variational theorem in the modeling of multilayered plates and shells." *Applied Mechanics Reviews*. 54(4), pp. 301–329. 2001. https://doi.org/10.1115/1.1385512

[8] Carrera, E. "Historical review of zig-zag theories for multilayered plates and shells." *Applied Mechanics Reviews*. 56(3), pp. 287–308. 2003. https://doi.org/10.1115/1.1557614

[9] Carrera, E., Giunta, G. "Refined beam theories based on unified formulation." *International Journal of Applied Mechanics*. 2(1), pp. 117–143. 2010. https://doi.org/10.1142/S1758825110000500

[10] Demasi, L. "∞^3 hierarchy plate theories for thick and thin composite plates: the generalized unified formulation." *Composite Structures*. 84, pp. 256–270. 2008. https://doi.org/10.1016/j.compstruct.2007.08.004

[11] Piskunov, V. G., Goryk, A. V., Lyakhov, A. L., Cherednikov, V. N. "High-order model of the stress–strain state of composite bars and its implementation by computer algebra." *Composite Structures*. 48, pp. 169–176. 2000. https://doi.org/10.1016/S0263-8223(99)00091-4.

[12] Piskunov, V. G., Goryk, A. V., Cherednikov, V. N. "Modeling of transverse shears of piecewise homogeneous composite bars using an iterative process with account of tangential loads. 1. *Construction of model.*" *Mechanics of Composite Materials*. 36(4), pp. 287-296. 2000. https://doi.org/10.1007/BF02262807

[13] Piskunov, V. G., Goryk, A. V., Cherednikov, V. N. "Modeling of transverse shears of piecewise homogeneous composite bars using an iterative process with account of tangential loads. 2. Resolving equations and results." *Mechanics of Composite Materials*. 36(6), pp. 445-452. 2000. https://doi.org/10.1023/A:1006798314569

[14] Cherednikov, V. M., Voskobiinyk, O. P., Cherednikova, O. V. "Про визначення параметрів напружено-деформованого стану сталезалізобетонних балочних елементів." (On the determination of stress-strain state of composite beam elements.) *Academic journal. Industrial Machine Building, Civil Engineering. Poltava National Technical Yuri Kondratyuk University*. 33(3), pp. 279-287. 2012. (in Ukrainian). URL: http://www.nbuv.gov.ua/old_jrn/natural/Znpgmb/2012_33/279.pdf

[15] Kumari, P., Kapuria, S., Rajapakse, R. K. N. D. "Three-dimensional extended Kantorovich solution for Levy-type rectangular laminated plates with edge effects." *Composite Structures*. 107, pp. 167-176. 2014. https://doi.org/10.1016/j.compstruct.2013.07.053

[16] Su, Y.-Y., Gao, X.-L. "Analytical model for adhesively bonded composite panel-flange joints based on the Timoshenko beam theory." *Composite Structures*. 107, pp. 112-118. 2014. https://doi.org/10.1016/j.compstruct.2013.07.018

[17] Wang, X., Shi, G. "A simple and accurate sandwich plate theory accounting for transverse normal strain and interfacial stress continuity." *Composite Structures*. 107, pp. 620-628. 2014. https://doi.org/10.1016/j.compstruct.2013.08.033

[18] Tornabene, F., Fantuzzi, N., Viola, E., Batra, R. C. "Stress and strain recovery for functionally graded free-form and doubly-curved sandwich shells using higher-order equivalent single layer theory." *Composite Structures*. 119, pp. 67–89. 2015. https://doi.org/10.1016/j.compstruct.2014.08.005

[19] Mashat, D. S., Carrera, E., Zenkour, A. M., Al Khateeb, S. A. "Axiomatic/asymptotic evaluation of multilayered plate theories by using single and multi-points error criteria." *Composite Structures*. 106, pp. 393–406. 2013. https://doi.org/10.1016/j.compstruct.2013.05.047

[20] Khalili, S. M. R., Shariyat, M., Rajabi, I. "A finite element based global–local theory for static analysis of rectangular sandwich and laminated composite plates." *Composite Structures*. 107, pp. 177–189. 2014. https://doi.org/10.1016/j.compstruct.2013.07.043

[21] Groh, R. M. J., Weaver, P. M. "Static inconsistencies in certain axiomatic higher-order shear deformation theories for beams, plates and shells." *Composite Structures*. 120, pp. 231–245. 2015. https://doi.org/10.1016/j.compstruct.2014.10.006